This motion is realizable, although the gravitational effect on the motion is a function of the roll angle, ϕ. Roll orientation effects are important in the determination of the long period modes but do not affect the attitude modes appreciably. In the current case, with $\cos \alpha = 0.836$ and $\sin \alpha = 0.549$, stability-axis roll rate has the effect shown in Fig. 1. Increasing roll rate stabilizes the short period mode and destabilizes the Dutch roll mode; the latter becomes unstable at a roll rate of 14.5 deg/sec. These results assume no control-loop closures. Augmented damping would materially alter these numerical results, although the trend toward decreased stability with increasing roll rate still would occur.

Effect of Dynamic Pressure

Maintaining velocity magnitude while varying altitude causes significant changes in q and minor changes in M. Some effects of a $\pm 20{,}000$-ft altitude shift are considered here. Reducing the altitude by 20,000 ft increases q to 148 psf, and it increases the stability of the short period and Dutch roll modes. The roll rate at which instability occurs is about 17 deg/sec. Conversely, stability is reduced with increasing altitude. With a 20,000-ft increase, q is reduced to 27 psf, and the Dutch roll mode is slightly unstable, even with zero roll rate (the roots are located at ± 0.0007506, ± 0.6568). Increasing the altitude by 10,000 ft results in $q = 40$ psf. The Dutch roll is stable at this point (with zero roll rate), but it becomes unstable when $p_S = 8$ deg/sec. It is concluded that the stability-axis roll rate at which instability first appears increases as q increases.

Effect of Sideslip Angle

As shown by Table 3, the direct effect of nonzero sideslip angle on the eigenvalues is not large; however, nonzero β causes instability to occur at very low roll rates. The enlarged circle in Fig. 1 illustrates the effect of a β of 2° on the progression of the roots with stability-axis roll rate. The crossover to instability occurs when $p_S = 5$ deg/sec. An interesting result is that the short period mode, not the Dutch roll mode, becomes unstable as a result of the roll rate. Further examination indicates that the short period mode is destabilized when p_S and β have the same sign, but the Dutch roll mode is destabilized when p_S and β have opposite sign. There are insufficient data to indicate whether or not this is a general result; however, it is reasonable to expect differing behavior when the vehicle is side-slipped "into" or "out-of" the rolling motion. Decreasing β to 1° increases the crossover p_S to 10 deg/sec, while increasing β to 4° decreases the roll rate for instability to 3 deg/sec.

Conclusions

The effects of sideslip angle and angular rates have been demonstrated for a high-α flight condition using fully coupled linear equations of motion. It is shown that the stability of the free motion of the vehicle is sensitive to roll rate and that this sensitivity is magnified by nonzero sideslip angle. These results suggest that fully coupled linearized equations can be of value not only for the study of Space Shuttle stability and control, but for a better understanding of post-stall gyrations, incipient spin, and departure prevention for high-performance aircraft.

References

[1] Phillips, W.H., "Effect of Steady Rolling on Longitudinal and Directional Stability," TN 1627, June 1948, NACA.

[2] Abzug, M.J., "Effects of Certain Steady Motions on Small-Disturbance Airplane Motions," *Journal of the Aeronautical Sciences*, Vol. 21, Nov. 1954, pp. 749-762.

[3] Byushgens, G.S. and Studnev, R.V., "Dynamics of the Spatial Motion of an Aircraft," TT F-555, April 1969, NASA.

[4] Etkin, B., *Dynamics of Atmospheric Flight*, Wiley, New York, 1972.

[5] Porter, R.F. and Loomis, J.P., "Examination of an Aerodynamic Coupling Phenomenon," *Journal of Aircraft*, Vol. 2, Nov.-Dec. 1965, pp. 553-556.

[6] Johnston, D.E. and Hogge, J.R., "The Effect of Non-Symmetric Flight on Aircraft High Angle of Attack Handling Qualities and Departure Characteristics," AIAA Paper 74-792, New York, Aug. 1974.

Slide-Valve-Controlled Vectoring Nozzle

J. A. C. Kentfield*
University of Calgary, Calgary, Alberta, Canada

Introduction

SOME time ago, a brief description was given of a ventral-type vectoring nozzle with the flow through the ventral aperture, cut in the wall of the jet pipe, controlled by a slide-valve of curved cross-section conforming to that of the jet pipe.[1] More recently, ventral nozzles with slide-valve control of the ventral orifice were described in further detail.[2] The prime advantages of slide-valve control of the ventral flow are a minimal increment in engine cross-sectional area, compared with that of a nonvectoring engine and simplicity; there is only one major moving part, the slide-valve, associated with the ventral orifice. The advantages of ventral as distinct from other types of vectoring nozzle have been discussed, in relation to a particular mission study, by Gill.[3] The ventral-type vectoring nozzle with slide-valve control appears to be suitable only for engines which are not augmented in the lift mode. Lift mode augmentation creates severe cooling problems with the slide-valve and flow guide-vanes.

This Note presents recently obtained experimental data relating to the aerodynamic performance, including the vectoring capability, of a slide-valve-controlled ventral outflow system. A major factor complicating the design of all ventral vectoring nozzles is the need to provide vector control with the entire engine flow passing through the ventral opening.

Thrust Vector Control

It is particularly important, with ventral nozzles, to arrange for a measure of thrust vector control in the lift mode with the full engine flow passing through the ventral aperture. Vector control, in an elementary ventral nozzle, solely by differential variation of the aft and ventral exit areas, results, due to the geometry of such an arrangement, in a fundamental thrust reduction. With the axes of the two flows at right angles, this reduction has a maximum value of just under 30% when the flow deflection angle θ is 45°; for $\theta = 0°$ and $\theta = 90°$ the reduction is zero. These points are apparent from Fig. 1 from comparison of the curves for the elementary and ideal cases. Figure 1 was established from simple resolution of the thrust forces resulting from outflow through the propulsion and ventral apertures of hypothetical ventral vectoring nozzles.

Full vector control over the range $60° \leqslant \theta \leqslant 90°$ with the entire engine flow passing through the ventral orifice, with the initial flow at 45° when the slide valve begins to open, is suf-

Received February 3, 1975; revision received February 28, 1975.

Index categories: VTOL Aircraft Design; VTOL Missions and Transportation Systems; VTOL Powerplant Design and Installation.

*Associate Professor, Mechanical Engineering Department. Member AIAA.

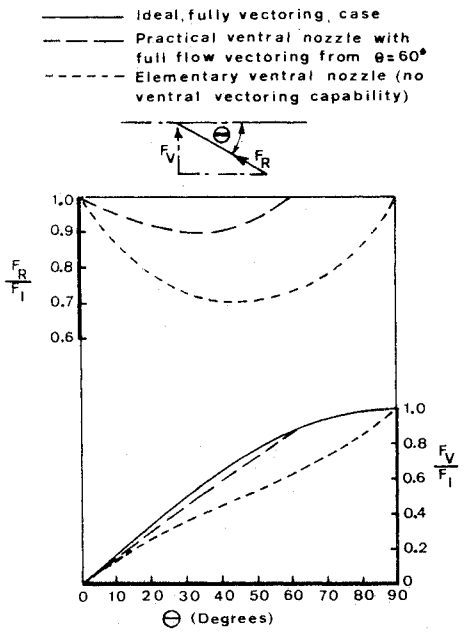

Fig. 1 Fundamental thrust characteristics of ideal, practical, and elementary ventral vectoring nozzles. F_I = ideal thrust (perfect vectoring), F_R = resultant thrust, F_V = vertical component of F_R.

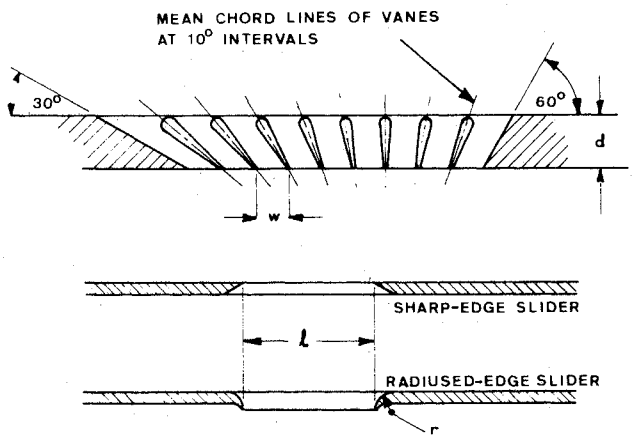

Fig. 2 Schematic arrangement of the flat working face flow model and alternative forms of slider. Airfoil and alternative flat plate guide vanes have the common chord lines shown. $d/w=1.6$, $\ell/w=4.0$, $r/w=0.5$.

ficient to substantially eliminate the difficulty (as can be seen from the curves for the practical case in Fig. 1). In practice, in order to assist with aircraft control in the hovering mode, it appears to be desirable to provide vectoring for $\theta > 90°$.

Flow Model

The flow model represented only the ventral opening region of the full vectoring nozzle. With a ventral-type vectoring nozzle, the portion of the system comprising the nozzle used for propulsion in the normal flight mode is conventional. The mechanism for closing the propulsion nozzle can take the form of blocker doors,[1,3] as often used in thrust reversing systems, or it can be of the star closure type described by Gill.[3]

The flow model, which was supplied with low-pressure air from a plenum chamber, is shown schematically with details of the geometry in Fig. 2. The pressure differential across the model was such that the flow Reynolds number $\approx 3 \times 10^4$ based on the jet efflux velocity and the distance w between adjacent vane trailing edges. Two sets of guide vanes were used; one set, shown in Fig. 2, consisted of airfoil cross-section vanes while, for the other, the vanes were of the flat plate

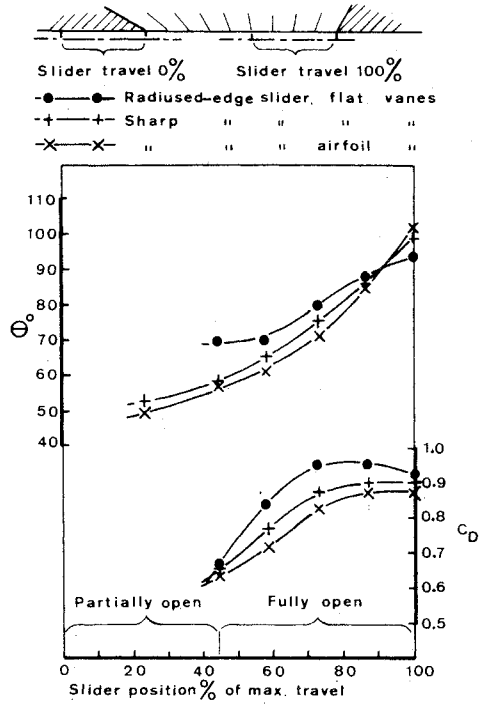

Fig. 3 Experimentally obtained performance characteristics of the model slide-valve-controlled vectoring system.

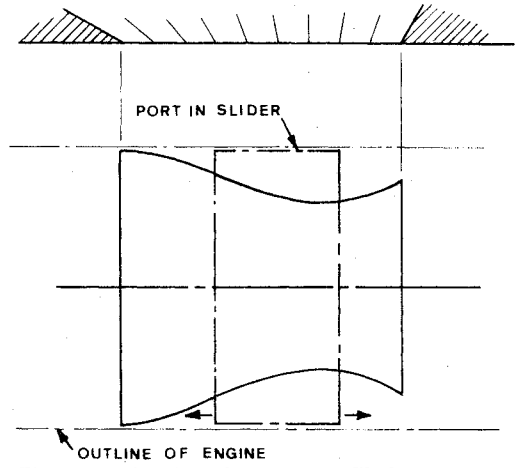

Fig. 4 First approximation of aperture profile for constant effective exit area when the entire engine flow passes through the ventral opening. Airfoil cross-section vanes and sharp edged slider configuration.

type. Two alternative slider configurations were also tested; one with a sharp edged opening in the slider, the other with the leading and trailing edges curved to a radius r where: $r=w/2$. The guide vanes were all of equal span: no attempt was made to tailor the aperture width to ensure a constant effective exit area over the vector range with the entire flow passing through the ventral opening, an essential feature of a slide-valve-controlled, ventral, vectoring nozzle.

Results

Results of the experiments are presented in Fig. 3 in the form of flow deflection, or vector, angle θ and corresponding discharge coefficient C_D vs slider position. The flow deflection angle was obtained by flow visualization; C_D was deduced from measurements of the volumetric flow rate. The values of C_D were based on the exposed flow area of the model (i.e., the product of the length, in the fore-and-aft direction, of the opening in the slider multiplied by the span of the vanes) less 10% to take into account the blockage, due

to the finite-thickness of the vane trailing edges.

It can be seen from Fig. 3 that the test using the slider with the radiused leading and trailing edges resulted in a generally higher discharge coefficient than was obtainable with the sharp edged slider, but only at the expense of vectoring capability. The vectoring range was greatest using the slider with sharp leading and trailing edges in conjunction with the airfoil-shaped vanes.

The experimentally obtained C_D-slider position relationships, for the uniform aperture width model, allow first approximations to be made of the required vane-span distributions necessary to ensure that a constant effective exit area will prevail over the range of operation in which the entire flow passes through the ventral opening. This has been done for the case of greatest practical interest, that with airfoil cross-section vanes used in conjunction with the sharp-edged slider; the result is shown in Fig. 4.

Conclusions

It was concluded that in general, vectoring nozzle with a slide-valve-controlled ventral opening appears to be feasible from the viewpoint of internal and external aerodynamics. It was further concluded that a range of vectoring between 10° forward to 30° aft of vertical with the entire flow passing through the ventral exit, essential for efficient operation of the nozzle and adequate aircraft control, is well within the capabilities of the device. A prediction of the thrust coefficient, based on realistic operating conditions (critical pressure ratio, Mach No. = 0.3 in the jet pipe), of the most practical configuration featuring airfoil cross-section vanes and a sharp-edged slider yielded a value of 0.95. Allowances were made for losses due to flow turning in the stream approaching the nozzle guidevanes, an effect absent from the model, flow over the guide vanes and divergence of the jet; the latter was based on observations of the flow paths in the efflux of the model nozzle.

Focussing of the thrust vectors, as depicted elsewhere,[2] was not investigated in the experiments. Failure to achieve a precise, singular, focussing effect may, or may not, be desirable: it would result in the focus of the thrust vectors tracing out a locus, which would be a function of slider position, instead of possessing a unique location independent of slider position. It would require more sophisticated tests than those reported here to investigate rigorously this aspect of the performance.

References

[1] Kentfield, J. A. C., "Nozzles for Jet-Lift V/STOL Aircraft," *Journal of Aircraft*, Vol. 4, July-Aug. 1967, pp. 283-291.

[2] Kentfield, J. A. C., "Comment on: Advanced Technology Thrust Vectoring Exhaust Systems," *Journal of Aircraft*, Vol. 12, No. 8, pp. 690-691.

[3] Gill, J. C., "Advanced Technology Thrust Vectoring Exhaust Systems," *Journal of Aircraft*, Vol. 11, Dec. 1974, pp. 764-770.

Vertical Tail Size Needed for a Coordinated Turn Reversal

E. Eugene Larrabee*
Massachusetts Institute of Technology, Cambridge, Mass.

THIS Note presents a simplified analysis of the vertical tail load required to reverse the direction of a coordinated turn. The load is proportional to the product of the tip helix angle and the aircraft weight, but is independent of the speed of flight. It may therefore set a lower limit on the acceptable vertical tail size for satisfactory turn coordination, in low-speed flight, particularly for sailplanes and STOL airplanes.

Presented as Paper 74-1004 at the AIAA/MIT/SSA 2nd International Symposium on the Science and Technology of Low Speed and Motorless Flight, Cambridge, Massachusetts, September 11-13, 1974; submitted February 14, 1975; revision received March 26, 1975.

Index category: Aircraft Handling, Stability, and Control.

*Associate Professor of Aeronautics and Astronautics. Member AIAA.

Analysis

The rate of change of heading in a coordinated level turn is given by

$$d\psi/dt = g \tan \phi \; V \tag{1}$$

where ψ and ϕ are the usual Euler angles, V is the flight speed, and g is the acceleration of gravity. During turn reversals the time derivative of the heading rate is therefore

$$d^2\psi/dt^2 = (g/V)\sec^2\phi(d\phi/dt)$$

As the aircraft rolls through wings level attitude, the rate of change of heading becomes identical to the angular acceleration about the Z stability axis, and the vertical tail must supply a moment

$$Y_v \ell_v = -I_z(dR/dt) = -mk_Z^2(g/V)\;(d\phi/dt) \tag{2}$$

where Y_v is the tail load (positive to starboard), ℓ_v is the tail moment arm, k_Z is the radius of gyration about the aircraft Z axis, and R is the yaw rate.

The rolling wing will generate a yawing moment given by

$$N = \tfrac{1}{2}\rho V^2 Sb\left[C_{n_\delta}\delta + C_{n_p}\frac{b}{2V}\frac{d\phi}{dt}\right]$$

To the extent that the lift distribution remains nearly elliptic during rolling (the additional lift due to rolling approximately cancels the additional lift due to control deflection), and to the extent that the lift per unit span, dL/dy, at a typical spanwise station, y, is rotated through the local helix angle (as would be true of wing sections having good leading-edge flow), the yawing moment may be approximated by

$$N = \tfrac{1}{2}\rho V^2 Sb\left[-\frac{C_L}{8}\right]\frac{b}{2V}\frac{d\phi}{dt} \tag{3}$$

and this additional (adverse) yawing moment also has to be supplied by the vertical tail. The total tail load turn reversals is therefore

$$Y_v = -\frac{1}{\ell_v}\left[mk_Z^2\frac{g}{V}\frac{d\phi}{dt}\right.$$

$$\left. + \tfrac{1}{2}\rho V^2 SB(1/8C_L)(b/2V)(d\phi/dt)\right]$$

or

$$Y_v = -mg(b/\ell_v)\left[2(k_Z/b)^2 + \tfrac{1}{8}\right]\left[(b/2V)\;(d\phi/dt)\right] \tag{4}$$

Alternatively, Eq. (4) may be expressed as a vertical tail volume coefficient requirement

$$(VTVC) = \frac{C_L}{C_{L_V}}\frac{q}{q_v}\left[2(k_z/b)^2 + 0.125\right]\left[(b/2V)(d\phi/dt)\right] \tag{5}$$

where C_L is the airplane lift coefficient, C_{L_V} is the maximum lift coefficient of the vertical tail, q is the flight dynamic pressure, and q_v is the dynamic pressure averaged over the vertical tail.

Discussion

A typical light airplane has the following characteristics:

$$\ell_v/b = 0.45,\; k_Z/b = 0.25$$